Research Article GU J Sci 35(2): 558-565 (2022) DOI: 10.35378/gujs.826774

Gazi University

Journal of Science

http://dergipark.gov.tr/gujs

Design and Fabrication of Compact Microstrip Low-pass Filter with Thin Film Technique for Wideband Applications

Resat TUZUN[1], Nursel AKCAM[2], Tayfun OKAN[2,*]

[1]*ASELSAN, Ankara, Turkey*
[2]*Gazi University, Engineering Faculty, Electrical Electronic Engineering Department, 06570, Ankara, Turkey*

Highlights

- This paper focuses on the design and analysis of a microstrip low-pass filter.
- Thin film technique is used to fabricate the proposed filter design.
- Sharp attenuation rate and high stopband attenuation level is obtained.

Article Info

Received: 17 Nov 2020
Accepted: 10 May 2021

Keywords

Low-pass filter
Microstrip filter
Thin film technique
C-band

Abstract

This paper introduces a compact microstrip low-pass filter (LPF) with a very sharp rejection. The proposed LPF is designed to be used for electronic warfare in defense industry. It has 62 dB/GHz attenuation rate, 10 GHz of stopband width and 48.6 dB of stopband attenuation. Moreover, it also has a wide passband and has a high cut-off frequency (f_c) of 6 GHz. The designed filter has been fabricated using alumina (Al_2O_3) substrate and titanium-gold (Ti-Au) coating on top of that with thin film technique in a clean room. The experimental measurements of the proposed LPF show great agreement with the simulation results, which validates that the presented filter is convenient to be used for applications up to C-band in electronic warfare systems.

1. INTRODUCTION

Microstrip filters gain importance for many RF applications like wireless communications and microwave/millimeter wave systems, as these systems demand lower loss, smaller size and higher performance. These superconductor filters with low insertion loss can also be used to harvest the frequency bands and to enhance the performance and sensitivity of devices such as multi-channel RF systems.

Many different filters were proposed in the past studies [1-3] for different purposes. Depending on the usage purpose of the filter, it is also important to select the right frequency band that is necessary for the operation of noise elimination. There are many studies available on literature [3-11], where low-pass filters (LPF) are designed and analyzed. But in most of those studies, the proposed filters have a narrow passband width and a cut-off frequency between 1 GHz to 2.5 GHz. In very few studies [7-10], the presented LPFs have a cut-off frequency value above 4 GHz. However, in those studies [7-10] the obtained attenuation rate values and stopband attenuation levels are relatively low, which are undesired outcomes for such filters.

Thin film microstrip filters have been studied before in different frequency bands [12-17], and successful results are obtained in these studies. In [12], the design and fabrication of a microstrip band-pass filter based on quadruplet geometry is reported, where the filter resembles elliptic function near passband and Chebyshev filter in the stopband. Multi-band bandstop filters are designed by using embedded I-stubs within a microstrip structure in [15] at 2.5/6.78 GHz, whereas in [16] High Temperature Superconductor (HTS) is used for the fabrication of the bandstop filter for L-band applications and it is reported that HTS has better performance than their gold-based counterparts. Bandpass filter is designed in [17] by the

*Corresponding author, e-mail: tokan@gazi.edu.tr

integration of cavities on thin film technology. The performance of the proposed filter is compared with a standard coupled lines filter and higher attenuation and lower insertion loss values are observed.

The size of the filter structure is another parameter that has attracted the attention of many researchers in the last decade. Many different techniques are proposed in [18-21] to minimize the filter size. Triangular stubs with low characteristic impedance values are introduced in [18] to miniaturize a microstrip filter. Wang et al. [19] proposed a half mode technique to reduce the size of the bandpass filter. Besides its compact size, wide stopband characteristics are reported in this study. Another filter size miniaturization technique is presented in [20], where the size of an LPF is minimized by using defected ground structure and multilayer methods. Conventional hairpin resonators are further minimized in [21] by loading a capacitor between the ends of the resonators.

In this paper, we have designed, fabricated and tested microstrip LPFs that can be used in many space, radar or wireless communication applications. Among the designed filters the most suitable one with high attenuation rate and high stopband attenuation is fabricated. Alumina (Al_2O_3) as a substrate is coated with titanium (Ti) and gold (Au) thin films to fabricate the designed microstrip C-band filter.

2. DESIGN OF THE MICROSTRIP FILTER

The design procedure of a microstrip LPF generally starts by determining the frequency response, fluctuation in the passband, number of reactive elements and some other parameters necessary for filter design. The filter design equations that includes Chebyshev polynomial order, wavelength and cut-off frequency parameters are used in this design process, and the performance of the designed filter is analyzed by using S-parameters. All these aforementioned parameters of LPF prototype are then converted to L-C circuit elements to provide the desired cut-off frequency and source impedance of 50 Ohms for most microstrip implementations.

Sonnet software program is preferred to design the filter, where all the filters are designed with lumped LC elements. The optimum filter dimensions and filter response are obtained by entering the necessary parameters to the system: filter type, approach method, cut-off frequency, source impedance and filter order. The dielectric constant and thickness of the substrate are chosen as $\varepsilon_r = 9.8$ and $d = 10\ mil$ $(254\ \mu m)$, respectively. Alumina is preferred as the substrate, since it is one of the most suitable material that can be used with thin film technique. Furthermore, to have a better impedance matching, source impedance is selected as 50 Ω for the designed microstrip LPF. Instead of elliptic or maximally flat, the approach type is chosen as Chebyshev; since it gives better results and cut-off performance.

The frequency response characteristic of the designed filter obtained by the Sonnet software program is depicted in Figure 1, where the insertion loss and return loss values are represented by blue and yellow colored curves, respectively. The designed microstrip LPF is desired to have around 6 GHz cut-off frequency and around 50 dB stopband attenuation value. That is why a marker is put at 6.6 GHz to analyze the effect of change in filter order on attenuation. It is observed that the most desired attenuation rate and stopband attenuation values are obtained with 19^{th} order of the filter. As can be seen in Figure 1, the attenuation value is 57.9 dB at 6.6 GHz for 19^{th} order. Since, the experimental measurements tend to give worse results than simulations; the 57.9 dB attenuation value is expected to be around 45 dB in real life measurements. In Figure 2, the final layout of the designed filter can be seen with its optimum dimensions, where all the dimensions are expressed in the unit of mil.

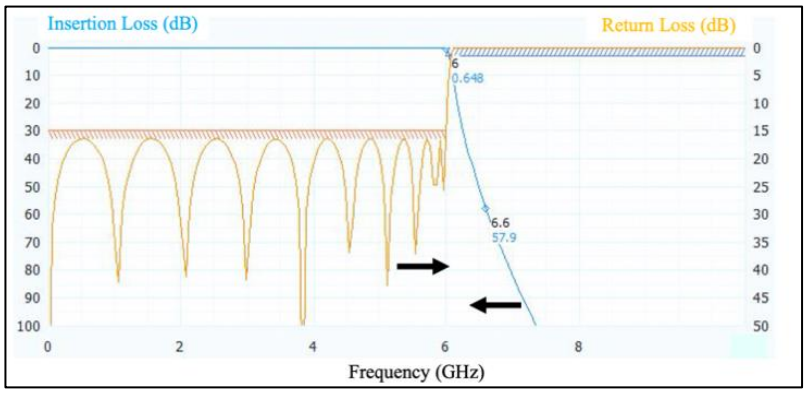

Figure 1. *Frequency response of the filter obtained by Sonnet software program*

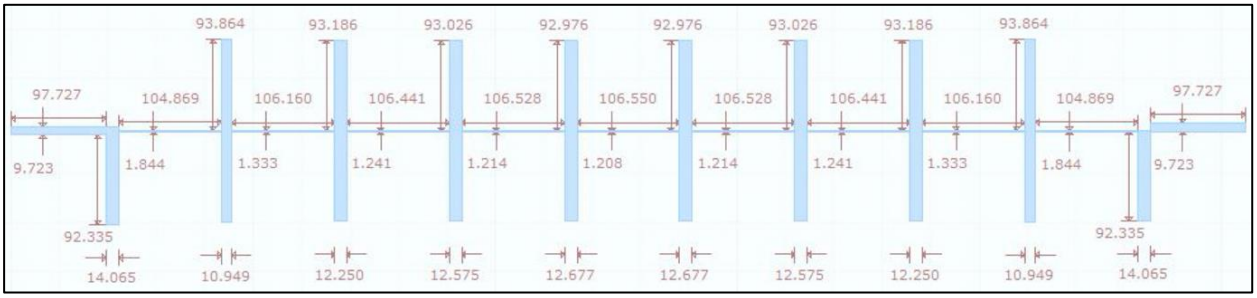

Figure 2. *Layout and dimensions of the designed filter*

Once the microstrip low-pass Chebyshev type filter is designed, Axiem Tool (a tool of AWR software program) is used in order to reach the return loss (S_{11}) and insertion loss (S_{21}) parameters. The values obtained with this tool are close to the experimental measurements. By means of this simulation program (Figure 3), more realistic results are obtained than the ones obtained in the prior design stage (Figure 1). As can be seen in Figure 3, the attenuation value at 6.6 GHz is 46.34 dB; however, in Figure 1 it was observed as 57.9 dB. Similarly, the loss value between DC to 6 GHz in design process and simulation are obtained as 0.648 dB and 3.66 dB, respectively. Since these parameters are all in the acceptable range, it is determined to fabricate the designed filter.

In the next step, the L-C model of the resonator is extracted as given in Figure 4. The impedance values or in other words the L and C values of the equivalent circuit are derived for an N^{th} order Chebyshev polynomial filter with the help of Equations (1) and (2)

$$P_{LR} = \frac{P_{inc}}{P_{load}} \ , \tag{1}$$

$$P_{LR} = 1 + k^2 T_N^2 \left(\frac{w}{w_c}\right) \tag{2}$$

where P_{LR} represents the power loss ratio, P_{inc} and P_{load} represent the power at the source and the power delivered to the load, respectively. Moreover, $T_N(x)$ is the Chebyshev polynomial, w_c is the cut-off frequency, N is the filter order, and k is a parameter determined from the passband ripple value. The inductance and capacitance values for the equivalent circuit are determined as L_1=1.49 nH, L_2=1.59 nH, L_3=1.61 nH, L_4=1.61 nH, L_5=1.61 nH, L_6=1.61 nH, L_7=1.61 nH, L_8=1.59 nH, L_9=1.49 nH, C_1=1.16 pF, C_2=1.67 pF, C_3=1.71 pF, C_4=1.72 pF, C_5=1.72 pF, C_6=1.72 pF, C_7=1.72 pF, C_8=1.71 pF, C_9=1.67 pF, C_{10}=1.16 pF. Circuit simulated results show great agreement with the EM simulated results, which indicates the validity of the L-C circuit model.

Up to three levels of subheadings can be used (2., 2.1., 2.1.1. etc). For further degrees of subheadings, do not use numbers, but simply give the heading in italics (*Heading* instead of 2.1.1.1. Heading). Single blank

line must be left between titles, subtitles and the text body as in the paragraph separation. *Italic font* can be used for emphasis within the text.

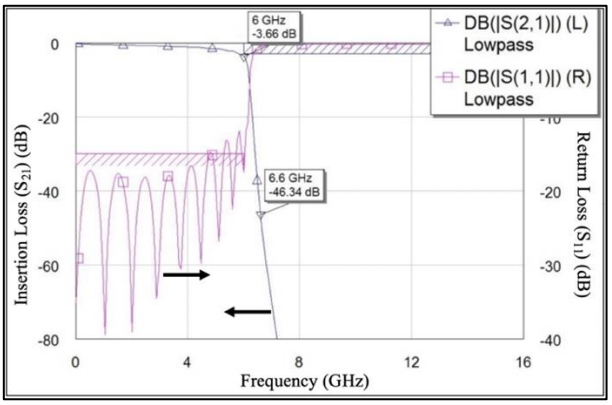

Figure 3. *Frequency response of the designed filter obtained with AWR Axiem simulation*

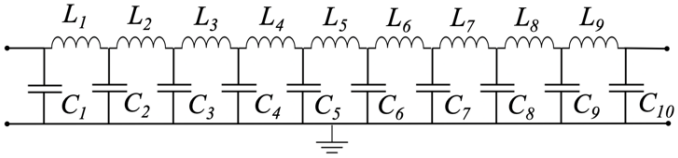

Figure 4. *LC equivalent circuit*

3. MEASUREMENTS AND RESULTS

All the necessary conditions are provided before starting the thin film fabrication process; which are 1) having a clean room (at least Class-6) and 2) covering all the light sources found inside the clean room with yellow-filter. Moreover, it is important to emphasize that both sides of the substrate have the same coating process. There is a titanium layer on top of alumina, with a thickness of 600 nm; and on top of that there is a gold layer with a thickness of 5 μm.

In order to start the fabrication, firstly the substrate is coated with the photoresist as seen in Figure 5(a). This process is done to both sides by a centrifuge with a slew speed of 2000 rpm and 200 rpm/s acceleration. Each face is preheated with 60 C^o for 1 minute after coating. The design pattern is then written on the substrate by using direct writing technique with a UV writing head. Next, a bathing chemical is used for photoresist decontamination of the UV exposed substrate as seen in Figure 5(b). After the last heating process, the substrate is immersed in gold etchant and titanium etchant, respectively. As the final step, the substrate is totally removed from the resistor and laser cut with wet dicing technique.

The fabricated filters are compact in size with the dimensions of $25.8 \times 5.6\ mm^2$ ($1.015 \times 0.22\ inch^2$). The three fabricated microstrip LFPs are tested with an experimental setup using a Vector Network Analyzer (VNA), as shown in Figure 5(c). Those results are transferred to AWR software program to make a better comparison and validate the simulation results.

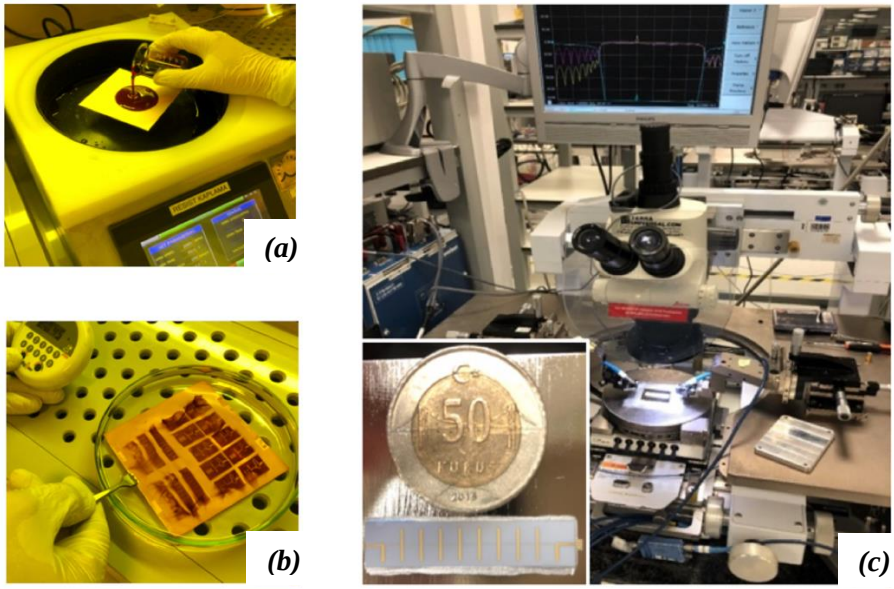

Figure 5. *Fabrication process: a) coating of substrate with photoresist, b) photoresist decontamination process, and c) experimental measurement setup with the layout of the proposed filter*

Fabricated filters are numbered and tested individually in the test setup with VNA. All the obtained results are overlapped on one graph in order to observe whether the experimental outcomes of the fabricated filters coincide with each other and with the simulation results. The S_{11} and S_{21} results are examined together in Figure 6, where the simulation result is labeled as "EM Structure 1" and the results for the three fabricated filters are labeled as "1", "2" and "3", respectively. As seen from Figure 6, the return loss curves coincide properly with each other. The minimum return loss value obtained from the simulation result was -12.15 dB, whereas it is around -13.35 dB in the passband for the fabricated filters. Furthermore, the return loss of the fabricated filter in the stopband is also shown in Figure 6, which is very close to 0 dB.

The cut-off frequencies of the fabricated filters are placed at 6.003 GHz, so the filters have a relatively wide passband width. Besides that, the insertion loss was measured as 0.96 dB in the simulation. On the other hand, for the fabricated filters, attenuation starts at 6.003 GHz and the passband ripple level from DC to 5.8 GHz is 4.1 dB, which is a little higher than expected. However, this ripple level is acceptable; since the filter has a wide passband. The stopband is reached from 6.6 to 16.5 GHz with an attenuation level higher than 48 dB. The attenuation rate is measured as 62 dB/GHz, where the dimensions of the compact proposed filter is $25.8 \times 5.6\, mm^2$ with a thickness of 262 µm. All the aforementioned outcomes identify that successful results are obtained and the proposed filter is reproducible.

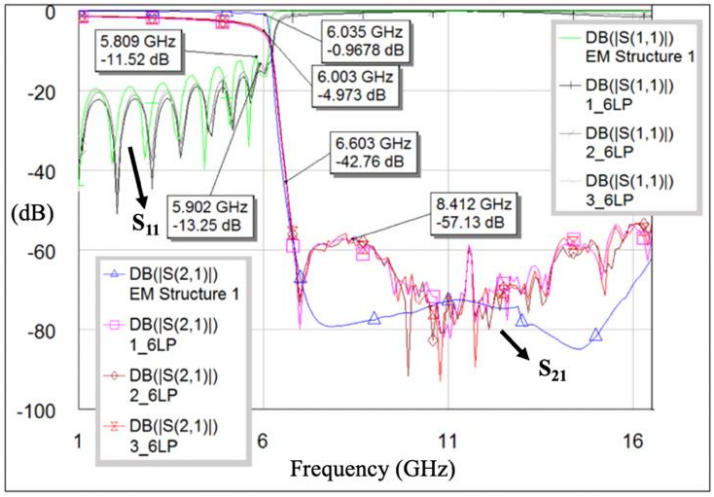

Figure 6. *Simulation and measurement results of the proposed filter*

The frequency response of both the fabricated filters and the response obtained from the simulation are matching and successive results are obtained with the proposed LPF especially when compared with the studies [7-9] having similar cut-off frequencies. As shown in Table 1, the attenuation rate of the proposed filter is sharper than the studies in [6, 8-10], maximum attenuation level in stopband is better than all the reported studies in [5-10], and the physical dimension of the proposed filter is smaller than the reported filters in [5-8]. The proposed filter is designed and fabricated on a substrate material that has the highest dielectric constant, when compared to other studies in Table 1. Using a high dielectric constant substrate results a reduction in filter size and an increase in design frequency range [18]. However, despite this size reduction, the presented filter is not the most compact in size as no further minimization techniques are applied. On the other hand, the filters in [5-10] were manufactured with conventional microelectronic technologies without any additional process, whereas thin film technology is utilized in the manufacturing process of this study. Applying thin film technique provides compactness, reduces loss and realizes highly selective filters [2]. This has a positive effect on the success and accuracy of the results obtained in experimental measurements.

Table 1. *Comparison with other state-of-arts in literature*

Work	Cut-off freq. (GHz)	Attenuation rate (dB/GHz)	Stopband attenuation (dB)	Size (mm×mm)	Dielectric constant	Filter type
[7]	5.2	-	20	24×14.7	4.4	LPF
[8]	4.0	42.5	20	19.83×8.64	2.2	LPF
[9]	8.0	11.4	20	14.1×2.1	2.2	LPF
[10]	8.7	7	10	12.9×1.56	2.2	LPF
[5]	2.28	121.4	20	19.8×11	3.38	LPF
[6]	2.49	49	20	17.37×15.1	2.2	LPF
Proposed	6.003	62	48.6	25.8×5.6	9.8	LPF

4. CONCLUSION

In this study, a microstrip LPF that has a cut-off frequency of 6 GHz is proposed. Attenuation rate and maximum attenuation level in stopband values are 62 dB/GHz and 48.6 dB, respectively. For a LPF operating at this cut-off frequency, these are very successive results. The length, width and height of the proposed filter is 25.8 mm, 5.6 mm, 262 μm, respectively. Furthermore, the minimum line thickness value of the designed filter is 1.2 mil. Filter is designed by AWR Sonnet program and fabricated with thin film technique. The three fabricated filters are tested between 1-16.6 GHz frequency band. The simulation and experimental results are compared with respect to insertion loss and return loss values. In this comparison since all the values are seem to be matched, one can say that the filters are produced in accordance with the design and the fabricated filter is convenient to be used in applications up to C-band in defense industry.

CONFLICTS OF INTEREST

No conflict of interest was declared by the authors.

REFERENCES

[1] Jadeja, R., Faldu, A., Trivedi, T., Chauhan, S., Patel, V., "Compensation of harmonics in neutral current using active power filter for three phase four wire system", Gazi Journal of Science, 31(3): 846-861, (2018).

[2] Alboon, S. A., Karar, A. S., Mahariq, I., Al-Sheikh, B., "Reconfigurable thin film filter for compensating AOI deviation effects using LC coupled cavities", Optics Communications, 456, 124672, (2020).

[3] Ekhteraei, M., Hayati, M., Hossein Kazemi, A., Zarghami, S., "Design and analysis of a modified rectangular-shaped lowpass filter based on LC equivalent circuit", AEU - International Journal of Electronics and Communications, 126, 153290, (2020).

[4] Vala, A., Patel, A., Goswami, R., Mahant, K., "Defected ground structure based wideband microstrip low-pass filter for wireless communication", Microwave and Optical Technology Letters, 59: 993-996, (2017).

[5] Makki, S. V., Ahmadi, A., Majidifar, S., Sariri, H., Rahmani, Z., "Sharp Response Microstrip LPF using Folded Stepped Impedance Open Stubs", Radioengineering, 22: 328-332, (2013).

[6] Yang, R. Y., Lin, Y. L., Hung, C. Y., Lin, C. C., "Design of a compact and sharp rejection low-pass filter with a wide stopband", Journal of Electromagnetic Waves and Applications, 26: 2284-2290, (2012).

[7] Wang, L., Yang, H. C., Li, Y., "Design of compact microstrip low-pass filter with ultra-wide stopband using SIRs", Progress in Electromagnetics Research Letters, 18: 179-186, (2010).

[8] Hayati, M., Sheikhi, A., "Microstrip lowpass filter with very sharp transition band using T-shaped, patch, and stepped impedance resonators", ETRI Journal, 35: 538–541, (2012).

[9] Khezeli, M. R., Hayati, M., Lotfi, A., "Compact wide stopband lowpass filter using spiral loaded tapered compact microstrip resonator cell", International Journal of Electronics, 101: 375-382, (2014).

[10] Zhang, C. F., "Compact and wide stopband lowpass filter with novel comb CMRC", International Journal of Electronics, 96: 749-754, (2009).

[11] Moitra, S., Dey, R., Bhowmik, P. S., "Design and band coalition of dual band microstrip filter using DGS, coupled line structures and series inductive metallic vias", Analog Integrated Circuits and Signal Processing, 101: 77-88, (2019).

[12] Kant, R., Gupta, N., "Design and implementation of inverse legendre microstrip filter", Microwave and Optical Technology Letters, 59: 69-73, (2016).

[13] Nath, J., Ghosh, D., Maria, J. P., Kingon, A. I., Fathelbab, W., Franzon, P. D., Steer, M. B., "An electronically tunable microstrip bandpass filter using thin-film Barium-Strontium-Titanate (BST) varactors", IEEE Transactions on Microwave Theory and Techniques, 53: 2707-2712, (2005).

[14] Jeong, S.-M., Kang, Y., Lim, T., Ju, S., "Chemically Reactive Polyurethane-Carbon Nanotube Fiber with Aerogel-Microsphere-Thin-Film Selective Filter", Advanced Materials Interfaces, 5: 1-6, (2018).

[15] Zhang, W., Gu, J., Xu, G., Luo, L., Li, X., "Copper/benzocyclotene thin film technique based microstrip bandpass filter featured by thick dielectric layer for low insertion loss", Microwave and Optical Technology Letters, 62: 3695-3701, (2020).

[16] Nasraoui, H., Capobianco, A. D., Mouhsen, A., El-Aoufi, J., Mouzouna, Y., Taouzari, M., "Compact wideband band pass microstrip filter loaded by triangular split ring resonators", Microwave and Optical Technology Letters, 59: 3101–3107, (2017).

[17] Quijano, G. P., Carchon, G. J., Nauwelaers, B. K. J. C., Raedt, W., "Horizontal Integration of Cavity Filters on High-Resistivity Silicon Thin-Film Technology", IEEE Transactions on Microwave Theory and Techniques, 56: 2893-2901, (2008).

[18] Yu, J. J., Chew, S. T., Leong, M. S., Ooi, B. L., "New class of microstrip miniaturised filter using triangular stub", Electronics Letters, 37(19): 1169-1170, (2001).

[19] Wang, Y., Hong, W., Dong, Y., Liu, B., Tang, H. J., Chen, J., Yin, X., Wu, K., "Half Mode Substrate Integrated Waveguide (HMSIW) Bandpass Filter", IEEE Microwave and Wireless Components Letters, 17(4): 265–267, (2007).

[20] Boutejdar, A., Omar, A., Burte, E., Batmanov, A., Mikuta, R., "A new logarithmic method to minimize the size of low-pass filter using multilayer and defected ground structure technique", Microwave and Optical Technology Letters, 53(11): 2561–2566, (2011).

[21] Sagawa, M., Takahashi, K., Makimoto, M., "Miniaturized hairpin resonator filters and their application to receiver front-end MIC's", IEEE Transactions on Microwave Theory and Techniques, 37: 1991-1997, (1989).